Colloid Polym Sci (2008) 286:1135–1141
DOI 10.1007/s00396-008-1875-1

ORIGINAL CONTRIBUTION

The effect of PVP-*b*-PMAA block copolymer on morphologies control of calcium carbonate

Puyu Zhang · Xueli Zhong · Yun Chai · Yang Liu

Received: 2 July 2007 / Revised: 6 March 2008 / Accepted: 13 April 2008 / Published online: 6 May 2008

Abstract A novel double-hydrophilic block copolymer (DHBC) poly(vinyl pyrrolidone)–block–poly(methacrylic acid) (PVP-*b*-PMAA) was synthesized via reversible addition–fragmentation chain transfer polymerization. The structure of the resulting copolymer was characterized by ^{1}H nuclear magnetic resonance, and the molecular weight of the block copolymer was determined by gel permeation chromatography. The study of morphological control of calcium carbonate ($CaCO_3$) has been performed in the presence of the PVP-*b*-PMAA block copolymer. Various morphologies of $CaCO_3$ particles such as rhombohedral, multilayered, and aggregated with cavities can be produced by varying the copolymer concentrations. The all-obtained $CaCO_3$ particles were calcite, which was confirmed by either X-ray diffraction or Fourier transform infrared spectra. Such calcium carbonate/polymer hybrids with complex morphologies may find valuable applications in biomimic mineralization.

Keywords Reversible addition–fragmentation chain transfer (RAFT) · Double-hydrophilic block copolymers · Calcium carbonate · Morphogenesis

Introduction

The synthesis of inorganic materials with specific size, morphology, and superstructure has attracted considerable attention due to the obvious importance of the shape and texture of materials in determining their properties [1]. It is well-known that biominerals exhibit highly optimized materials properties, hierarchical structure, and complex forms and are synthesized at ambient temperatures in an aqueous environment [2]. Inspired by the biominerals, the biomimetic synthesis of patterned inorganic materials is attracting increasing interest. In particular, the morphosynthesis of calcium carbonate in the presence of organic templates/additives has been intensively investigated due to the abundance in nature and also its important industrial application in paints, plastics, rubber, and paper [3–4]. In the recent years, polyelectrolytes [5], dendrimers [6], and double-hydrophilic block copolymers (DHBCs) [7–9] have been used for the morphology control of $CaCO_3$.

DHBCs have attracted tremendous attention due to their unique properties in aqueous solution such as micelle formation and their interactions with specific molecules [10]. DHBCs consist of one hydrophilic block designed to interact strongly with the surfaces of inorganic minerals and another hydrophilic block that does not interact (or only weakly interacts) but mainly promotes solubilization in water. Owing to the separation of the binding and the solvating moieties, DHBCs are "improved versions" of polyelectrolyte homopolymers and turn out to be extraordinarily effective as crystal growth modifiers in crystallization control for inorganic salts such as calcium carbonate [11–15], calcium phosphate [16], barium sulfate [17–19], zinc oxide [20, 21], and other metal carbonates [22].

In the previous works, the most widely used DHBC for the purpose of controlling inorganic crystal morphology is poly (ethylene glycol)–block–poly(methacrylic acid) (PEG-*b*-PMAA). There were some other double-hydrophilic copolymers developed recently. For example, Basko and Kubisa

P. Zhang (✉) · X. Zhong · Y. Chai · Y. Liu
Institute of Fine Chemistry and Engineering,
College of Chemistry and Chemical Engineering,
Henan University,
Kaifeng 475001, People's Republic of China
e-mail: zhangpuyu@henu.edu.cn

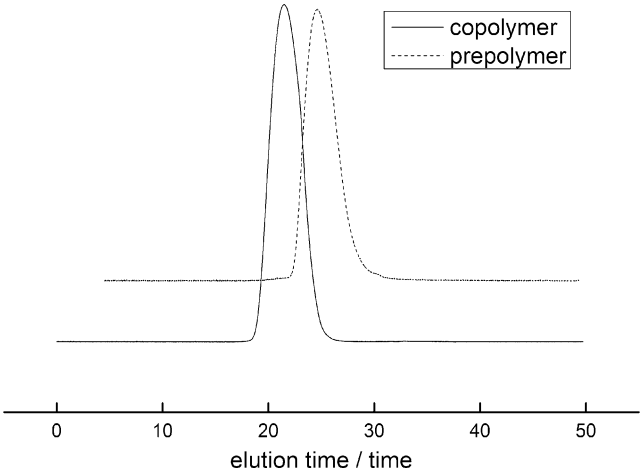

Fig. 1 GPC trace of copolymer PVP-*b*-PMAA

described the synthesis of graft copolymers that consist of the polyacetal backbone substituted with a carboxylic group and a poly(oxyethylene) side chain, and the efficiencies of the graft copolymers as modifiers for $CaCO_3$ were studied [23]. Cölfen studied the influence of phosphonated or phosphorylated DHBCs on mineral morphology control [24–26]. Yu also reported PEG-*b*-hexacyclen [27] and PEG-*b*-pGlu [28] as crystal growth modifiers.

The synthesis methods of DHBCs were comprehensively introduced in the review of Cölfen, including living anionic polymerization, living cationic polymerization, and living/controlled radical polymerization [10]. In the past decade, living/controlled radical polymerization has rapidly been developing as a powerful macromolecular engineering tool [29]. Reversible addition–fragmentation chain transfer (RAFT) polymerization is probably the most versatile tool of the prominent living/controlled free radical polymerization techniques to synthesize polymers with complex architecture ranging from block to star, as it is tolerant of a wide range of functionality in the monomer and solvent [30].

In numerous cases, PEG is used as the solvating block of a DHBC. In this study, considering that poly(vinyl pyrrolidone) is a hydrophilic polymer with its molecular weight, structure, property, and biocompability similar to protein [31], poly(vinyl pyrrolidone) (PVP)-*b*-PMAA as a novel DHBC was synthesized via RAFT polymerization, with PVP as the solvating block and PMAA as the functional block, respectively. The use of the PVP-*b*-PMAA copolymer as a modifier for the crystallization of $CaCO_3$ was also studied.

Experimental

Materials

N-Vinyl-pyrrolidone (NVP; Aldrich) and methacrylic acid (MAA; Kermel chemical agents, Tianjin) was vacuum distilled prior to use. 1-Phenylethyl dithiobenzoate (chain transfer agent, CTA) was synthesized according to the literature [32]. 2, 2′-Azbisisobutyronitrile (AIBN; Chemical agents, Shanghai) was recrystallized from methanol. $CaCl_2$, Na_2CO_3, and ethanol (Chemical agents) were used as received. The water used was deionized.

Synthesis of PVP

AIBN (0.3mmol) was added to a mixture of NVP (10ml), ethanol (20ml), and CTA (0.7mmol). The polymerization was carried out under a nitrogen atmosphere at 65 °C. After 4–5h, the reaction was terminated by dropping into acetone, and the resultant polymer was separated by filtration and dried in a vacuum oven.

Synthesis of PVP-*b*-PMAA

MAA (0.2mol) was first prepared to sodium salt and then mixed with deionized water (15ml). PVP (0.3mmol) and ethanol (15ml) were then added to the solution. The reactor was deoxygenated by purging with nitrogen, while the temperature of the oil bath remained constant at 85 °C. Then, a small amount of initiator AIBN dissolved in ethanol was added and heated at 85 °C for 10h, after which they were quenched and cooled to room temperature. The polymer was precipitated into acetone for the removal of the residual monomer.

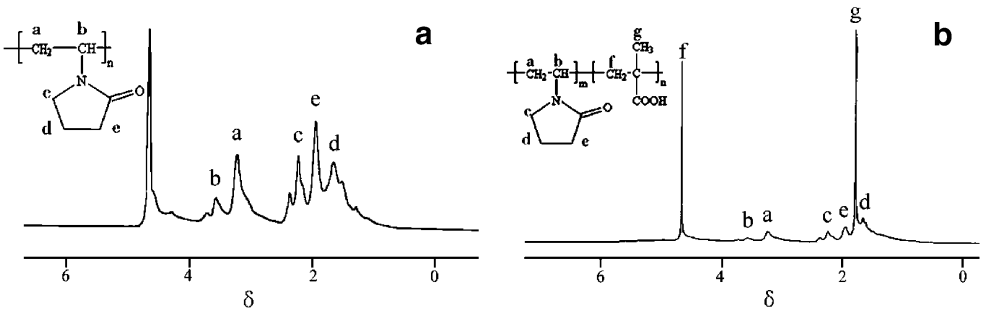

Fig. 2 ^{1}H NMR spectra of PVP (**a**), and PVP-*b*-PMAA (**b**) in D_2O

Table 1 Characterization of the polymer PVP-*b*-PMAA

Polymer	M_n ($\times 10^4$)[a]	M_w/M_n	Mn ($\times 10^4$)
PVP	1.36	1.26	3.47[b]
PVP-*b*-PMAA	2.88	1.42	3.84[c]

[a] Determined by GPC
[b] Determined by ^{1}H NMR spectroscopy: $M_{PVP}+M_{MAA}\times 244$
[c] Calculated by monometer conversion: $W_{MAA}/n_{PVP}\times$Conv.$+M_{PVP}$ monomer conversion 43.3%

Crystallization of $CaCO_3$

The precipitation of $CaCO_3$ was carried out in glass vessels at room temperature. Aqueous solutions of Na_2CO_3 (0.2M) and $CaCl_2$ (0.2M) were first prepared as stock solutions. In a typical procedure, a solution of Na_2CO_3 (0.2M, 1ml) was injected into an aqueous solution of PVP-*b*-PMAA (20ml), and the pH of the solution was adjusted to 10 by using NaOH. Then, a solution of $CaCl_2$ (0.2M, 1ml) was injected quickly into the pH-adjusted mixture under vigorous stirring by using a magnetic stirrer; this gave a final $CaCO_3$ concentration of 10mM. After 1min of stirring, the solution was covered and allowed to stand for 24h and then was centrifuged (4,000rpm, 10min) and washed with distilled water repeatedly and allowed to dry at room temperature. In the experiments, the concentrations of PVP-*b*-PMAA were varied from 0.05 to 1.0g l^{-1}.

Characterization

The ^{1}H nuclear magnetic resonance (NMR) spectra of the polymers were collected by using an AVANCE400M spectrometer (Bruker, Germany). The solution was prepared in D_2O and tetramethylsilane was used as the internal standard. The Fourier transform infrared spectra were recorded at room temperature on AVATAR360 (Nicolet, America) using KBr tablets. Gel permeation chromatography analyses (GPC) were performed on a Waters 515 HPLC pump equipped with an ultraviolet detector. The column was SHIMpack-800. $NaNO_3$ of 0.2M was used as an eluent at a flow rate of 0.5ml min^{-1}. Scanning electron microscopy (SEM) studies were conducted on a JSM5600LV (JEOL, Japan) microscope. Thermogravimetric analyses (TGA) were carried out on a TGA/SDTA 851e (Mettler, Switzerland) thermal analyst instrument with the nitrogen atmosphere at a heating rate of 10 °C min^{-1}. Powder X-ray diffraction (XRD) patterns were recorded on an X Pert Pro diffractometer (Philips, Holland).

Results and discussion

Polymer synthesis

RAFT is a well-known method for the controlled radical polymerization of water-soluble monomers. Therefore,

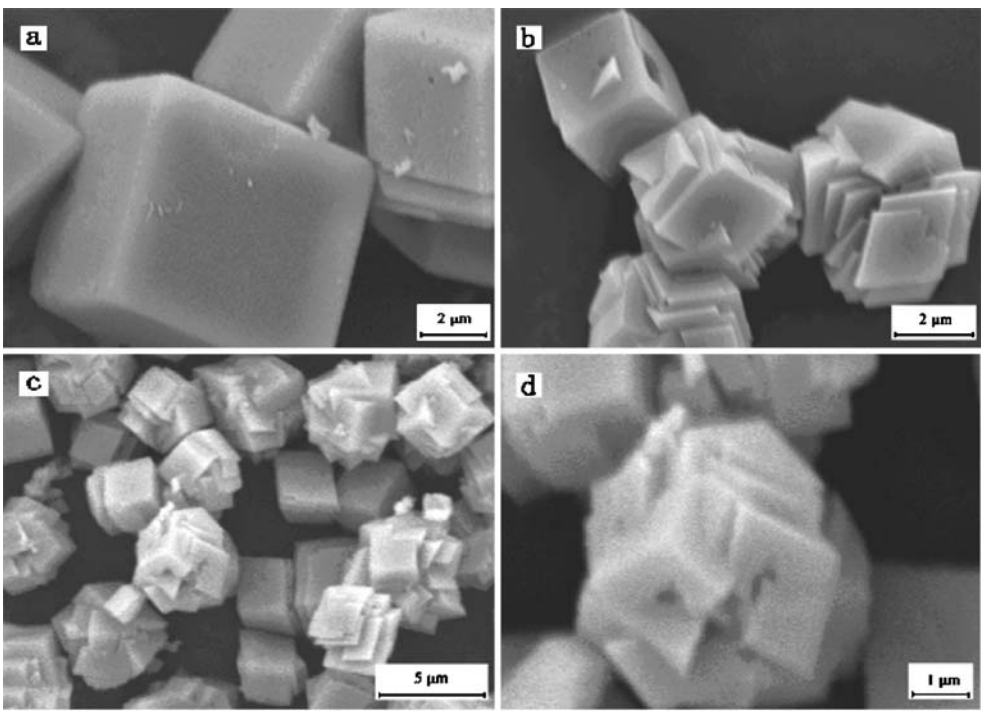

Fig. 3 SEM images of $CaCO_3$ particles obtained in the presence of no polymer (**a**), PVP (**b**), and PVP-*b*-PMAA (**c**, **d**), **d** is the high-magnifying image of the aggregated crystal of the **c**. [Polymer]=0.5 g l^{-1}, [$CaCO_3$]=10 mM, pH=10

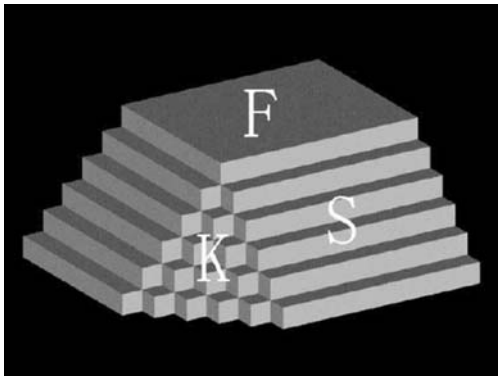

Fig. 4 A schematic representation of a crystal model exposing the F, S, and K planes

copolymers of NVP and MAA were synthesized via RAFT. Figure 1 shows the GPC trace of copolymer PVP-*b*-PMAA, which is a single peak without shoulders. The molecular weight of the copolymer was 28,800g mol^{-1}, and the molecular weight distribution index was as low as 1.42. These results indicated that the resulting product is the block copolymer of NVP and MAA rather than a simple mixture of the two blocks.

However, the analysis of the molecular weights of such DHBCs by GPC is hardly accurate because of the interactions between the functional groups and the column material [33]. The interactions often lead to a retardation of the polymer in the GPC column with respect to its corresponding hydrodynamic volume, resulting in a lower apparent molecular weight from GPC analysis. Thus, we used end-group analysis in ^{1}H NMR spectroscopy to determine the molecular weight of the PVP-*b*-PMAA copolymer and calibrate with GPC results. The ^{1}H NMR spectra are shown in Fig. 2. In the spectrum of PVP (Fig. 2a), peak a (3.18ppm) and peak b (3.70ppm) were assigned to the backbone protons (–CH_2– and –N–CH–, respectively), while peak c (2.36ppm), d (1.69ppm), and e (1.99ppm) were assigned to the three methylene groups on the pyrrolidone ring. After copolymerization, the –CH_3 of PMAA block appears at 1.71ppm, which was shown in Fig. 2b. Peak a and peak g were used for the end-group analysis, and the chain length ratio was 1/2. The results of both GPC and ^{1}H NMR analyses are listed in Table 1. As expected, the molecular weight given by GPC is much lower than the value evaluated by ^{1}H NMR, which is close to the result calculated by monomer conversion. These results showed that the ^{1}H NMR analyses could be used to determine the molecular weight of copolymers containing the functional group, as previously reported [34].

$CaCO_3$ crystallization

Figure 3 presents the typical SEM images of $CaCO_3$ particles obtained in the absence and presence of PVP or PVP-*b*-PMAA (both at 0.5g l^{-1}) under the same experimental conditions ($CaCO_3$ = 10mM; pH = 10). As expected, well-defined rhombohedral crystals were produced in the absence of polymeric additives (Fig. 3a), while multilayered crystals were obtained in the presence of PVP (Fig. 3b). When DHBC PVP-*b*-PMAA was used as an additive, the precipitate was found to consist of big

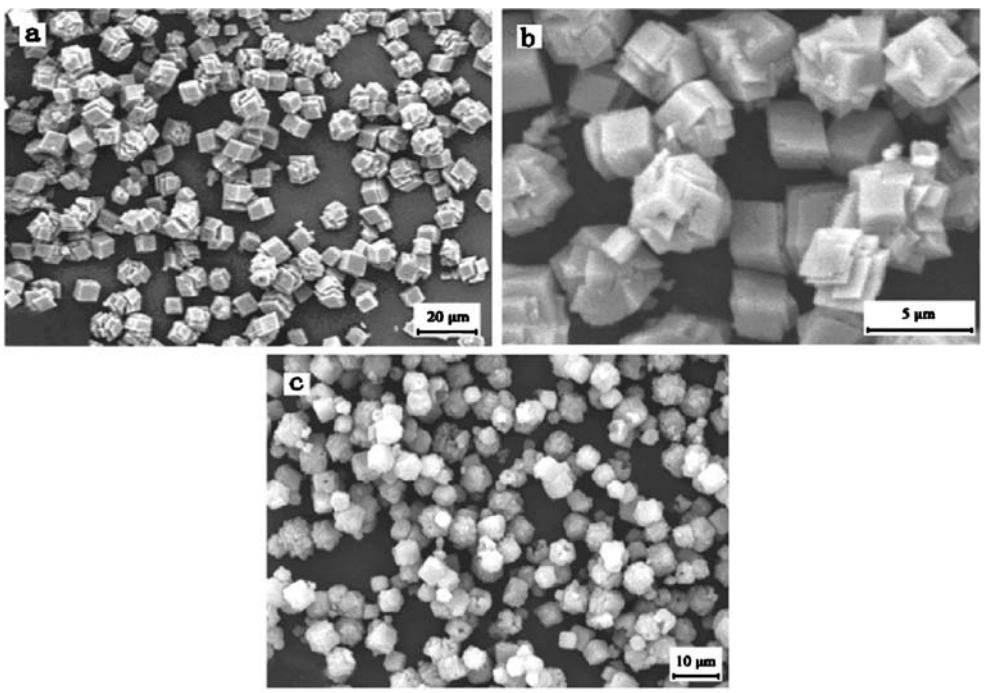

Fig. 5 $CaCO_3$ particles observed in the presence of PVP-*b*-PMAA. [Polymer]=0.05 (**a**), 0.5 (**b**), and 1.0 g l^{-1} (**c**). [$CaCO_3$]=10 mM, pH=10

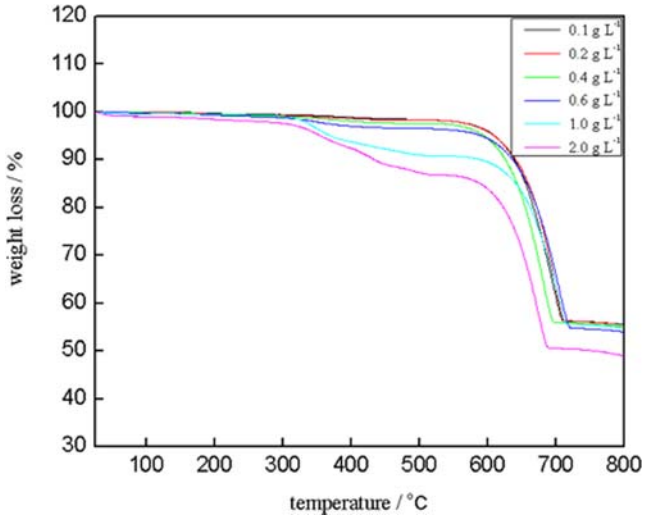

Fig. 6 TGA curves of $CaCO_3$ crystals formed in PVP-b-PMAA solutions. [Polymer]=0.1, 0.2, 0.4, 0.6, 1.0, and 2.0 g l^{-1}. [$CaCO_3$]= 10 mM, pH=10

aggregates and some rhombohedral crystals (Fig. 3c). The high magnifying SEM image of the aggregated crystals is shown in Fig. 3d.

A simple crystal model that is called the periodic bond chain is introduced to explain the changes of crystal morphologies (Fig. 4). In this crystal model, the planes of the crystals are classified into three groups, F (flat), S (stepped), and K (kinked) planes, as described by Hartman and Perdok [35]. The K and S planes can be considered as full of kinks and steps, respectively. It is obvious that the highest growth rate will be achieved at the K plane, then the S plane, and finally the F plane [36]. In the crystallization of $CaCO_3$, the polymer density on the newly developed K and S planes was higher than that on the original F planes of the crystals. As a high polymer density gives a lower growth rate, the relative growth rate on the F plane can be higher than those on the K and S planes [37]. As a consequence of inhibition by polymers, new crystal planes would be developed at the corners and edges of rhombohedral crystals, eventually creating morphology changes.

It is noteworthy that the multilayered structure was the only morphology in the presence of the PVP homopolymer, even at the higher PVP concentration (1.0g l^{-1}). This result supports that the presence of pure PVP has a poor effect on the crystallization of $CaCO_3$ and is not sufficient to modify the structure of $CaCO_3$ particles. However, the crystals' morphologies changed when the copolymers were used; different morphologies could be found depending on the copolymer concentration, which was varied from 0.05 to 1.0g l^{-1}. At the lower concentration of 0.05g l^{-1}, rhombohedra and multilayered crystals were both obtained (Fig. 5a). This indicates that at concentrations as low as 0.05g L^{-1}, the copolymer loses its ability to control the $CaCO_3$ morphology and modification. This may be ascribed to the lower polymer content incorporated in the product at the lower polymer concentration. A new type of morphology was produced due to the aggregated of multilayered crystals when the copolymer concentration was increased to 0.5g l^{-1} (Fig. 5b). At the highest copolymer concentration of 1.0g l^{-1}, the multilayered crystals totally disappeared, and only aggregated particles were left (Fig. 5c), suggesting a complete transformation from a multilayered structure to an aggregated structure.

To better illustrate the possible reason of the changes of the crystals morphologies from a lower concentration to a higher concentration, the TGAs of the obtained $CaCO_3$ was investigated and the results are shown in Fig. 6. All the TGA measurements show two decomposing processes. The first decomposing onset at 250 °C corresponds to the carbonization of the copolymer molecules, and the second one at 650 °C corresponds to the decomposition of $CaCO_3$ crystals. The polymer weight losses were nearly unobvious when the polymer concentration was 0.1 to 0.4g l^{-1}; when the concentration was increased to 0.6g l^{-1}, the weight loss approximately was 3.5 wt%, and with a further increase in the concentration to 1.0 and 2.0g l^{-1}, the polymer weight losses were 7.8% and 12.1%, respectively. These results indicate that the polymer content that participated in modifying the crystals' growth enhanced with the increasing copolymer concentration. At lower concentrations, the small amount of the copolymer preferentially adsorbed on the K and S planes, resulting in a multilayered morphology. With the increasing of the copolymer concentration, these

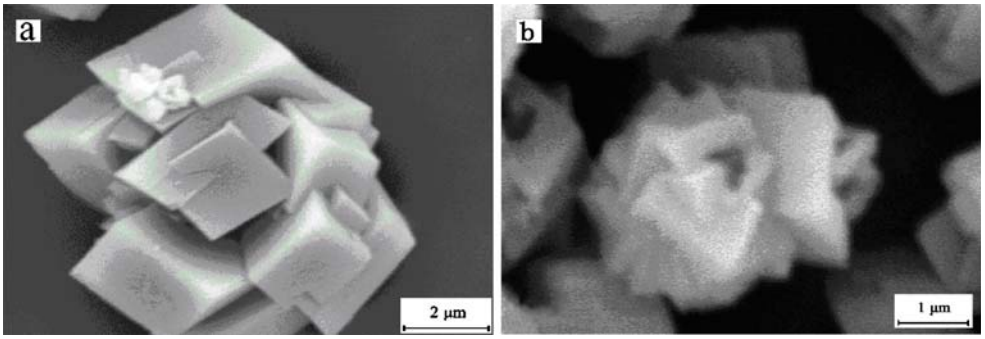

Fig. 7 SEM images of the forming process of the cavity in an aggregated crystal in the presence of PVP-*b*-PMAA. [Polymer]=0.5 (**a**) and 1 g l^{-1} (**b**). [$CaCO_3$]=10 mM, pH=10

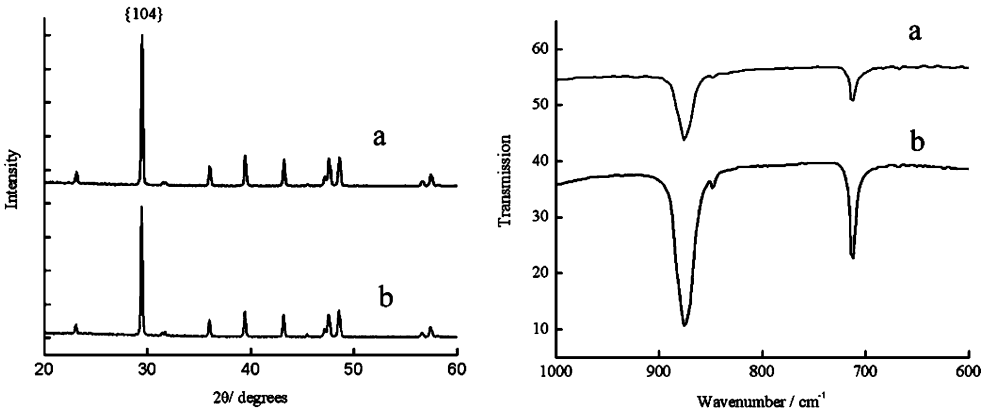

Fig. 8 XRD patterns (left) and infrared spectra (*right*) of $CaCO_3$ crystals obtained in the presence of PVP (*a*) and PVP-*b*-PMAA (*b*). [Polymer]=1 g l^{-1}, [$CaCO_3$]=10 mM, pH=10

planes could not bear the increased amount of the copolymer, which accumulated at the interspace of several $CaCO_3$ crystals; then, aggregated crystals were formed. It is noteworthy that at the highest copolymer concentration, some cavities were observed in the aggregated crystals (Fig. 5c and Fig. 7b). This could be explained that during the aggregation of the multilayered structure, the PMAA block adsorbed on the surface of the crystal and extended to the exterior area because of the electrostatic repulsion of the –COOH, resulting in the radiated distribution of multi-layered crystals along the center of the aggregated crystal (Fig. 7a). While, the growth rate of the inner aggregated crystals depressed because the polymer chain wrapped and finally grew into cavities (Fig. 7b).

Figure 8 shows the XRD results of the $CaCO_3$ crystals obtained in the presence of pure PVP and the copolymer PVP-*b*-PMAA. In both cases, the XRD pattern shows a sharp diffraction of {104} faces, which indicate that the crystal structure is composed of well-crystallized calcite crystals. The corresponding infrared spectrum (Fig. 7, right) exhibits sharp bands at 875 and 712cm^{-1}, characteristic of calcite [38], and this provides further evidence for the pure calcite composition of the products.

Conclusions

A novel DHBC PVP-*b*-PMAA with narrow molecular weight distribution was synthesized via RAFT living radical polymerization. While the GPC analysis of this DHBC was inaccurate to characterize the molecular weight of the copolymer, the ^{1}H NMR analyses could be used to determine the molecular weight of the copolymers containing the functional group. Owing to the double-hydrophilic character, the copolymer was applied as an effective crystal growth modifier of $CaCO_3$ particles. Various morphologies of $CaCO_3$ particles were produced by varying the polymer concentrations. The produced calcium carbonate particles with well-defined morphologies and sizes could have some interesting applications, e.g., as site-specific absorbers and chromatographic materials. It may be expected that the synthesized block copolymer could be applied to the crystallization control of many other inorganic salt systems.

References

1. Mann S (2000) Angew Chem Int Ed 39:3393
2. Wang TX, Rother G, Cölfen H (2005) Macromol Chem Phys 206:1619
3. Kato T, Sugawara A, Hosoda N (2002) Adv Mater 14:869
4. Meldrum FC (2003) Int Mater Rev 48:187
5. Gower LA, Tirrell DA (1998) J Cryst Growth 191:153
6. Naka K, Tanaka Y, Chujo Y (2002) Langmuir 18:3655
7. Qi LM, Cölfen H, Antonietti M, Li M, Hopwood JD, Ashley AJ, Mann S (2001) Chem Eur J 7:3256
8. Cölfen H, Qi LM (2001) Chem Eur J 7:106
9. Zhang DB, Qi LM, Ma JM, Cheng H (2002) Chem Mater 14:2450
10. Cölfen H (2001) Macromol Rapid Commun 22:219
11. Sedlak M, Antonietti M, Cölfen H (1998) Macromol Chem Phys 199:247
12. Cölfen H, Antonietti M (1998) Langmuir 14:582
13. Marentette JM, Norwig J, Stockelmann E, Meyer WH, Wegner G (1997) Adv Mater 9:647
14. Gao YX, Yu SH, Cong HP, Jiang J, Xu AW, Dong WF, Cölfen H (2006) J Phy Chem B 110:6432
15. Endo H, Schwahn D, Cölfen H (2004) J Chem Phys 120:9410
16. Antonietti M, Breulmann M, Goltner CG, Cölfen H, Wong KKW, Walsh D, Mann S (1998) Chem Eur J 4:2493
17. Qi LM, Cölfen H, Antonietti M (2000) Angew Chem Int Ed 39:604
18. Qi LM, Cölfen H, Antonietti M (2000) Chem Mater 12:2392
19. Cölfen H, Qi LM, Mastai Y, Borger L (2002) Crystal Growth Design 2:191
20. Oner M, Norwig J, Meyer WH, Wegner G (1998) Chem Mater 10:460
21. Taubert A, Kubel C, Martin DC (2003) J Phys Chem B 107:2660
22. Yu SH, Cölfen H, Antonietti M (2003) J Phys Chem B 107:7396
23. Basko M, Kubisa P (2004) J Polym Sci Part A Polym Chem 42:1189
24. Rudloff J, Antonietti M, Cölfen H, Pretula J, Kaluzynski K, Penczek S (2002) Macromol Chem Phys 203:627
25. Qi LM, Cölfen H, Mann S (2004) J Mater Chem 14:2269
26. Yu SH, Cölfen H, Tauer K, Antonietti M (2005) Nature Mater 4:51
27. Chen SF, Yu SH, Wang TX, Jiang J, Cölfen H, Hu B, Yu B (2005) Adv Mater 17:1461
28. Guo XH, Yu SH, Cai GB (2006) Angew Chem Int Ed 45:3977

29. Davis KA, Matyjaszewski K (2002) Adv Polym Sci 159:1
30. Stenzel-Rosenbaum M, Davis TP, Chen V, Fane AGJ (2001) J Polym Sci Part A Polym Chem 39:2777
31. Cui YD, Yi GB, Liao LW (2001) Synthesis and application of poly(vinyl pyrrolidone). Science, Beijing, p 38
32. Moad G, Chiefari J, Chong YK, Krstina J, Mayadunne RTA, Postma A, Rizzardo E, Thang SH (2000) Polym Int 49:993
33. Sedlak M, Cölfen H (2001) Macromol Chem Phys 202:587
34. He L, Zhang YH, Ren LX, Chen YM, Wei H, Wang DJ (2006) Macromol Chem Phys 207:684
35. Hartman P, Perdok WG (1955) Acta Cryst 8:521
36. Shen FH, Feng QL, Wang DM (2002) J Cryst Growth 242: 239
37. Markov IV (2003) Crystal growth and epitaxy, 2nd edn. World Scientific, Singapore
38. Falini G, Albeck S, Weiner S, Addadi L (1996) Science 271:67